DRC0028

Localized damping identification of a flat plate using relative phase of nearfield acoustics

Pitiphong Atibodhi[1,*], Chak Chantalakhana[2]

[1] The Sirindhorn International Thai-German Graduate School of Engineering (TGGS), King Mongkut's University of Technology North Bangkok (KMUTNB), 10800, Thailand
[2] Department of Mechanical Engineering, KMUTNB, 10800, Thailand

* Corresponding Author: pititphon.a-deme2014@tggs-bangkok.org

Abstract. In order to reduce amplitude of vibrating structures additional damping such as constrained-layer damping is being used to dissipate vibration energy at local and critical locations. To understand complex vibration modes of the structure due to inhomogeneous distribution of structural damping, the identification and characterization of the localized damping is necessary. The localized damping identification method is developed in this work. The method is applied to both numerical simulation and experimental analysis. The non-contact sound pressure transducers are used to eliminate mass loading due to use of accelerometers, two microphones are used to measure nearfield acoustic along a nodal line of an anti-symmetric mode. The nearfield acoustics response at a nodal line correlates to the locations and sizes of localized damping.

1. Introduction

The additional damping treatments such as constrained-layer damping (CLD) is often placed at the critical areas of the structure, to reduce and control structure vibration problem [1]. The efficient damping treatments can increase dissipation rate of vibration energy and improve vibration behavior of the structure. The placement of these damping treatments can derived from the optimization process [2], which lead to very local and critical locations of the vibrating structure. To identify the localized damping on the structure, experimental modal analysis is one of the standard experimental approaches to estimate damping ratio at each location on the structure which is time consuming to measure all points on the structure. Also the effects of transducer mass loading can alter the damping properties of the flexible structure, the use of non-contact sound pressure transducers can resolve the problems.

In this work, localized damping identification method is developed, where sound pressure transducers are used to measure nearfield acoustic along a nodal line of an anti-symmetric mode. In Section 2, the nearfield acoustic at nodes of a normal mode are described. In Section 3, the occurrence of complex vibration modes due to the localized damping and the phase distortion of the nearfield acoustic at a nodal line are related. In Section 4, the modal testing and the nearfield acoustic measurement were carried out on a rectangular plate. The experimental results were used to update and validate numerical Finite Element/Boundary Element (FE/BE) model. The structural FE model was validated and updated using experimental modal results. The coupled FE/BE model of a vibro-acoustic plate was validated for the plate vibrating at non-resonance and resonance frequency. The deviation between the measured acoustic pressure and from coupled FE/BE model are less than 10%. The localized damping identification method was applied on both numerical simulation and experimental analysis.

2. Nearfield acoustic at nodes of normal mode

The acoustic radiation from an infinite plate vibrating in a normal mode has been given in [3]. The radiation from an infinite plate vibrating in a standing wave mode at a single frequency with normal surface velocity η given by:

$$\eta(x,y) = \eta_0 \cos(k_{x0}x)\cos(k_{y0}y) \tag{1}$$

where k_{x0} and k_{y0} are the wavenumber in the x and y directions of the plate located in the $z = 0$. The distance between nodal lines on the plate in the x and y directions is given by:

$$\lambda_{x0}/2 = \pi/k_{x0}\ ,\ \lambda_{y0}/2 = \pi/k_{y0} \tag{2}$$

The conditions needed to solve this boundary value problem, to determine the pressure on the half-space above the plate [1], the pressure p must satisfy the Helmholtz equation ($\nabla^2\bar{p} + k^2\bar{p} = 0$), the fluid particle velocity $\dot{\omega}$ must satisfy Euler's equation ($i\dot{\omega}\rho_0\vec{v} = \vec{\nabla}p$) for $z \geq 0$, the fluid always stays in contact with the plate so the displacement of the fluid particles near the plate boundary and normal to the plate surface must be continuous ($\eta(x,y) = \dot{\omega}(x,y,z), at\ z = 0$) and there are no sources above the plate. With above conditions, the steady state pressure p radiated from a vibrating plate with surface velocity given in equation (1) can be obtained:

$$p(x,y,z) = \frac{\eta_0\rho_0 ck}{k_{z0}} e^{ik_{z0}z}\cos(k_{x0}x)\cos(k_{y0}y) \tag{3}$$

where ρ_0 is the fluid density, c is the speed of sound in the medium, k_{x0} and k_{y0} are the given wavenumbers of the modal pattern of the plate and k_{z0} is a function of them and the acoustic wavenumber k:

$$k_{z0} = \pm\sqrt{k^2 - {k_{x0}}^2 - {k_{y0}}^2} \tag{4}$$

as usual $k = \omega/c$, where ω is the radian frequency of the plate oscillation. When the nodal lines in either directions on the plate ($\lambda_{x0}, \lambda_{y0}$) are separated by less than a half of acoustic wavelength, k_{x0} and/or k_{y0} wavenumbers of the modal pattern is greater than k the acoustic wavenumber, the square root in equation (4) becomes:

$$k_{z0} = -i\sqrt{{k_{x0}}^2 + {k_{y0}}^2 - k^2} = ik'_{z0} \tag{5}$$

Where the argument of the square root is now positive and k'_{z0} is real. The pressure above the plate in equation (3) now becomes:

$$p(x,y,z) = \frac{-i\eta_0\rho_0 ck}{k'_{z0}} e^{-k'_{z0}z}\cos(k_{x0}x)\cos(k_{y0}y) \tag{6}$$

decaying exponentially away from the plate boundary. The adjacent regions of negative and positive velocity tend to cancel one another at nodal line area. By combining this acoustic wave propagating at nodal line area with the existing of complex mode, the localized damping identification using relative phase of nearfield acoustic near nodal line was developed in the next section.

The FE/BE formulation of structural-acoustic system has been given in [4] for coupled fluid-structural system in an open environment. It is assumed that structure is totally submerged to acoustic medium, the effect of the acoustic medium to the boundary can be neglected, and no coupling exists between the structural and acoustic damping.

The structural equations of motion:

$$[M_s]\{\ddot{u}_s\} + [C_s]\{\dot{u}_s\} + [K_s]\{u_s\} = \{f_s\} - [K_c]\{p_a\} \tag{7}$$

The acoustic equations of motion:

$$[M_a]\{\ddot{p}_a\} + [C_a]\{\dot{p}_a\} + [K_a]\{u_s\} + [M_c]\{\ddot{u}_s\} = \{f_s\} \tag{8}$$

The combined fluid-structure equations becomes:

$$\begin{bmatrix} M_s & 0 \\ M_c & M_a \end{bmatrix}\begin{Bmatrix} \ddot{u}_s \\ \ddot{p}_a \end{Bmatrix} + \begin{bmatrix} C_s & 0 \\ 0 & C_a \end{bmatrix}\begin{Bmatrix} \dot{u}_s \\ \dot{p}_a \end{Bmatrix} + \begin{bmatrix} K_s & K_c \\ 0 & K_a \end{bmatrix}\begin{Bmatrix} u_s \\ p_a \end{Bmatrix} = \begin{Bmatrix} f_s \\ f_a \end{Bmatrix} \tag{9}$$

where u_s is the structural displacement vector and p_a is the sound pressure vector of the acoustic field; f_s is the structural force vector and f_a is the sound source in the acoustic field; M_s and K_s are the structural mass and stiffness matrices, respectively; M_a and K_a are the acoustic mass and stiffness matrices, respectively; M_c and K_c are the coupling matrices of the structural-acoustic system. Equation (9) is asymmetric due to coupling between the structure and the acoustic field, it is symmetrized by using a variable transformation. Let a velocity potential q be defined such that

$$p = \dot{q} \tag{10}$$

Assuming harmonic time dependence, equation (9) can written in the form:

$$\begin{bmatrix} M_s & 0 \\ 0 & M_a \end{bmatrix}\begin{Bmatrix} \ddot{u}_s \\ \ddot{q} \end{Bmatrix} + \begin{bmatrix} C_s & K_c \\ -M_c & -C_a \end{bmatrix}\begin{Bmatrix} \dot{u}_s \\ \dot{q} \end{Bmatrix} + \begin{bmatrix} K_s & 0 \\ 0 & -K_a \end{bmatrix}\begin{Bmatrix} u_s \\ q \end{Bmatrix} = \begin{Bmatrix} f_s \\ \frac{f_a}{i\omega} \end{Bmatrix} \tag{11}$$

Because of Euler's equation, the pressure p and the velocities $\dot{u}_f$ can be obtained from equation (10) and following equation:

$$\dot{u}_f = -\frac{1}{\rho_0}\nabla q \tag{12}$$

The FE/BE simulation results of the vibro-acoustic plate shown in figure 1, a rectangular plate is free supported and vibrating at first normal mode. The acoustic filed at nodes of normal mode shown in figure 1(a) & figure 1(b), acoustic wave propagating from moving or active parts of structure propagate to the nodes area. A plot of acoustic pressure at a node at different heights show in figure 1(c), which can be devided into three regimes. The first two regimes have approximatley constant pressure level, and pressure decay in the third regime. The charaterization of nearfiled acoutic at nodes will perform at regime-1, which is more sensitive to acoutic wave propagating from adjacent area than regime-3 and less sensitive to environment distrubance.

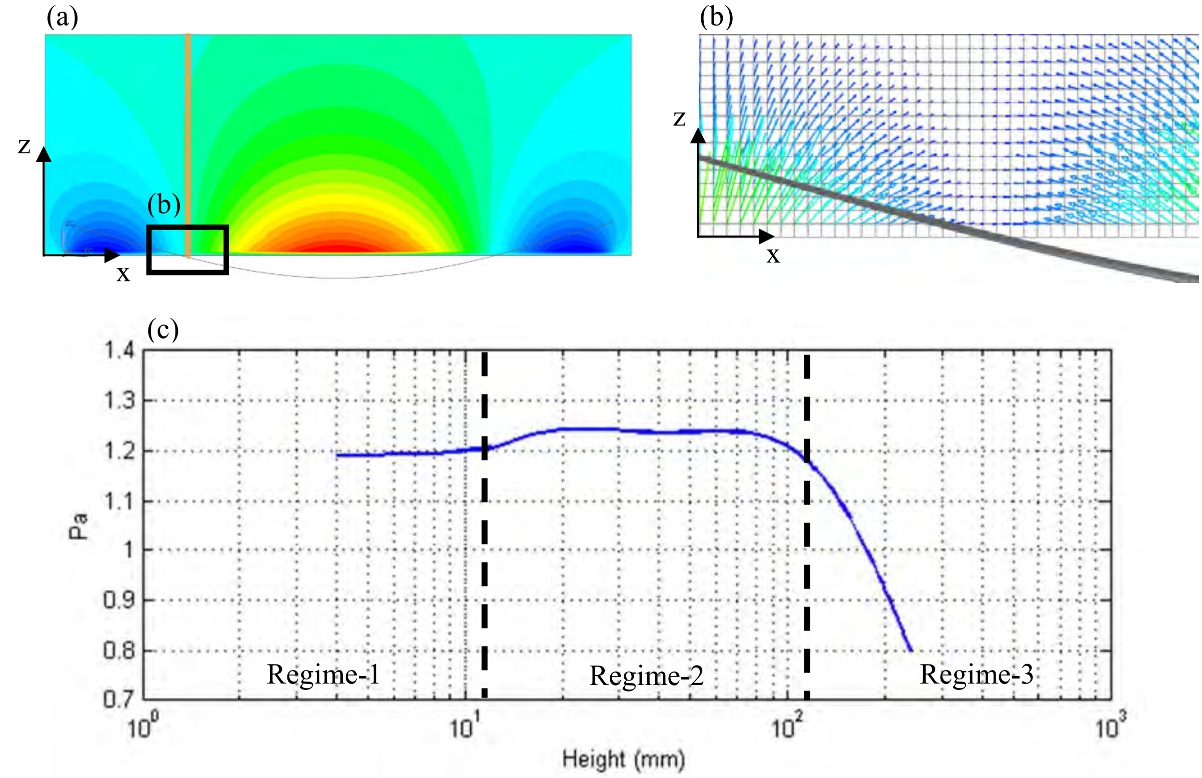

Figure 1. (a) Acoutic pressure field over the plate vibrating at 1st normal mode, and (b) acoustic intensity vector, (c) and acoustic pressure at a node at different heights.

3. Identification method of localized damping

The localized damping usually result in a non-proportional to the stiffness distribution which is the condition for complex modes to exist. As a result, each part of a structure vibrating in a complex mode will reach its own maximum deflection at a different phases. While a real mode is one in which the phase angles are all identically 0° or 180° so all parts of structure do reach their own maxima all at the same instant in the vibration cycle. If two adjacent areas close to the nodal line of normal mode have different localized damping, the acoustic wave propagating from these two area will reach nodes area at different instant of time.

Numerical simulation results of nearfield acoustic on the plate vibrating at an anti-symmetric mode or torsional normal mode shown in figure 2, the contour plot of signed amplitude of acoustic pressure. The positive pressure, zero pressure and negative pressure shown in red, green, blue colour respectively. The nearfield acoustic at a nodal line area was characterized at two section lines parallel to a nodal line and slightly offset from a nodal line, which is at the centre of the plate for this torsion mode. For without damping case (real mode), figure 2(a) & figure 2(c), the phase angles are all identically 0° or 180° at all location along upper (dot) and lower (dash) section. The constrained-layer added to a model to simulate localized damping case shown in figure 2(b), high phase distortion can be observed at localized damping location. The details of FE/BE model is described in Section 5.

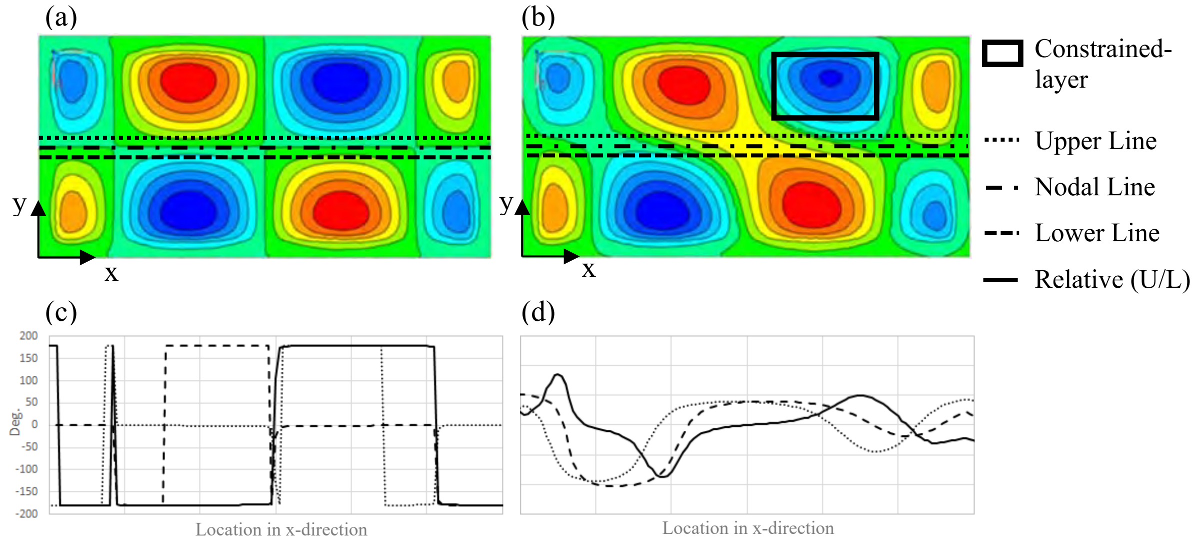

Figure 2. Acoustic singed pressure over a plate vibrating at torsional normal mode (a) without and (b) with localized damping. Acoustic pressure phase at nodal line area (c) without and (d) with localized damping.

The relative phase between upper (dot) line and lower (dash) line shown in solid line in figure 2(c) & figure 2(d). In the experiment, the relative phase can be obtained by using a pair of microphones measure acoustic pressure along a nodal line. This new method is developed for operational analysis or output-only analysis, a technique for characterizing localized damping of a test structure using only response data of the structure whose inputs are unknown and/or difficult to measure. The distortion of relative phase could be observed at the localized damping area, same as seen on acoustic phase contour plot, but this relative phase method require only two microphones and small number of measurement points at nodal line areas.

4. Test setup

The dimensions of the rectangular aluminum plate being studied are 0.600 x 0.250 x 0.008 m., the material is aluminum 6061 (69 GPa Young's modulus, 0.33 Poison's ratio, 2700 kg/m^3). The plate was suspended using 4 suspensions, as shown in figure 3(a), to simulate the free boundary conditions. The plate was excited at different locations, for modal testing and plate vibrating at the third torsional mode the excitation location is at (559, 205) mm from the origin, for out of plane vibrating at non-resonance mode is at (300, 125) mm from the origin as shown in figure 3(c) using 2025E The Modal Shop modal shaker. The excitation direction was perpendicular to the plate surface. The responses of the plate were measured using one Kistler 8770A50 impedance head and three Kistler 8704A50 accelerometers for modal testing and two B&K 4958 microphones for nearfield acoustic measurement, the data were collected using an LMS spectrum analyzer. For modal testing, the three accelerometers were attached on the bottom surface of the plate. For nearfield acoustic measurement, the two microphones were placed at the end of aluminum bar arm which is movable in three axes as shown in figure 3(a). For calculating relative phase between upper and lower lines of nodal area as discussed in Section 4, a pair of microphones were set to measure acoustic field along the nodal line area of the third torsional mode of the plate as shown in figure 3(b).

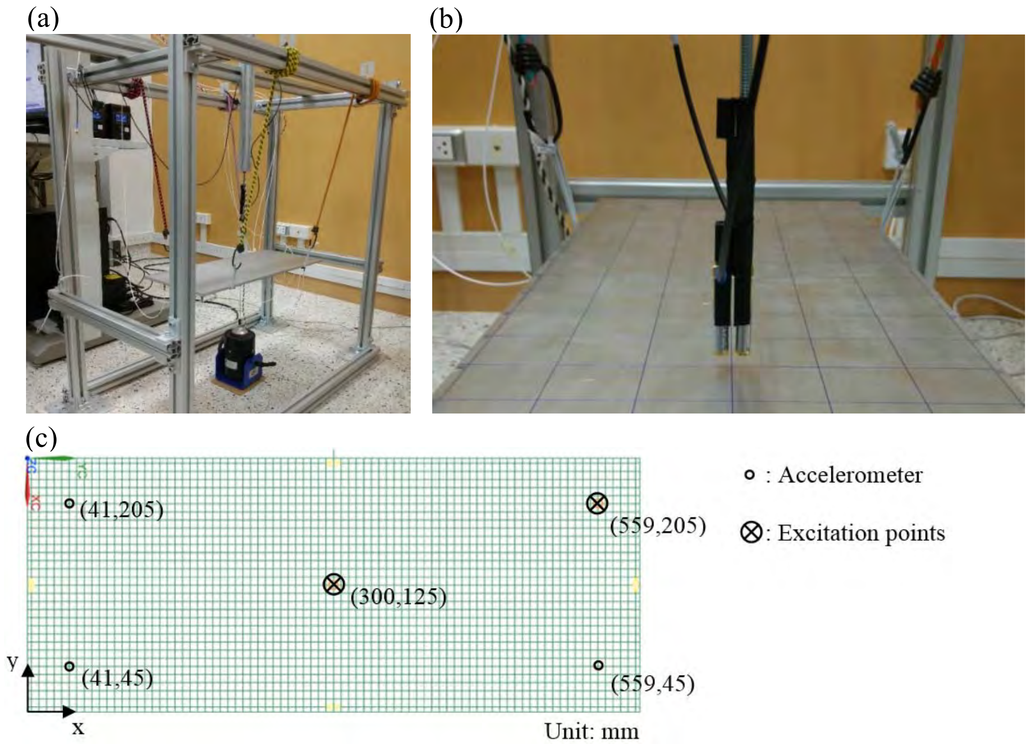

Figure 3. (a) Test setup for the modal testing and nearfield acoustic measurement, (b) a pair of microphones, (c) excitation points & sensors locations.

5. Numerical and experimental results

Numerical simulation is conducted for structural modal analysis and vibro-acoustic analysis using commercial FE software Simcenter 11.0, the FE/BE model shown in figure 4. The FE/BE model was validated using experimental results on both the plate vibrating at non-resonance mode and at resonance mode. Then the different placement configurations of localized inhomogeneous damping on a plate were studied using the FE/BE model to characterize nearfield acoustic. The Constrained-Layer Damping (CLD) was applied to a structure to simulate localized damping, which model by the viscoelastic layer (1 mm thickness, 40 GPa Young's modulus, 0.4 Poison's ratio, 1200 kg/m^3 and 0.3 damping ratios) and the constraining layer (0.3 mm thickness, same material as a base structure) as shown in figure 4.

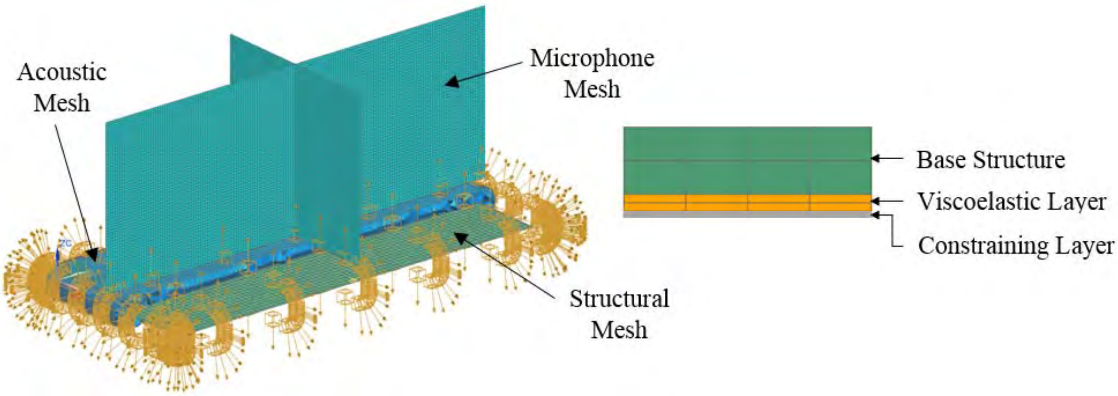

Figure 4. Vibro-acoustic FE/BE model and Constrained-Layer Damping (CLD) model

The structural FE model was validated and updated first by using experimental results from modal testing. The measured modal parameters (natural frequency, damping ratio) were extracted from four sets of measured FRFs from the three accelerometers and one impedance head. The damping ratio was applied to each natural frequency, the driving point FRF comparing between experimental and updated FE model shown in figure 5.

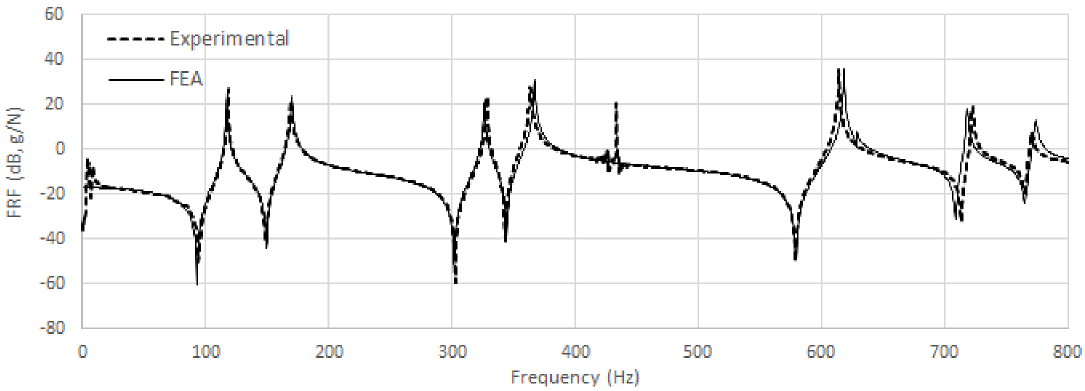

Figure 5. Driving point FRF by modal testing and FE method.

Then the coupled FE/BE model of a vibro-acoustic plate was validated on two cases. The first case is the plate vibrating at non-resonance mode at 20 Hz away from the first bending mode at 117 Hz. The shaker excitation point is at the center of the plate with 3 N force. Figure 6 shows comparisons between FE/BE simulation and measurement results. The maximum deviation of plate acceleration and acoustic pressure from FE/BE model, compare with measurement results, are 4.5% and 6.5% respectively.

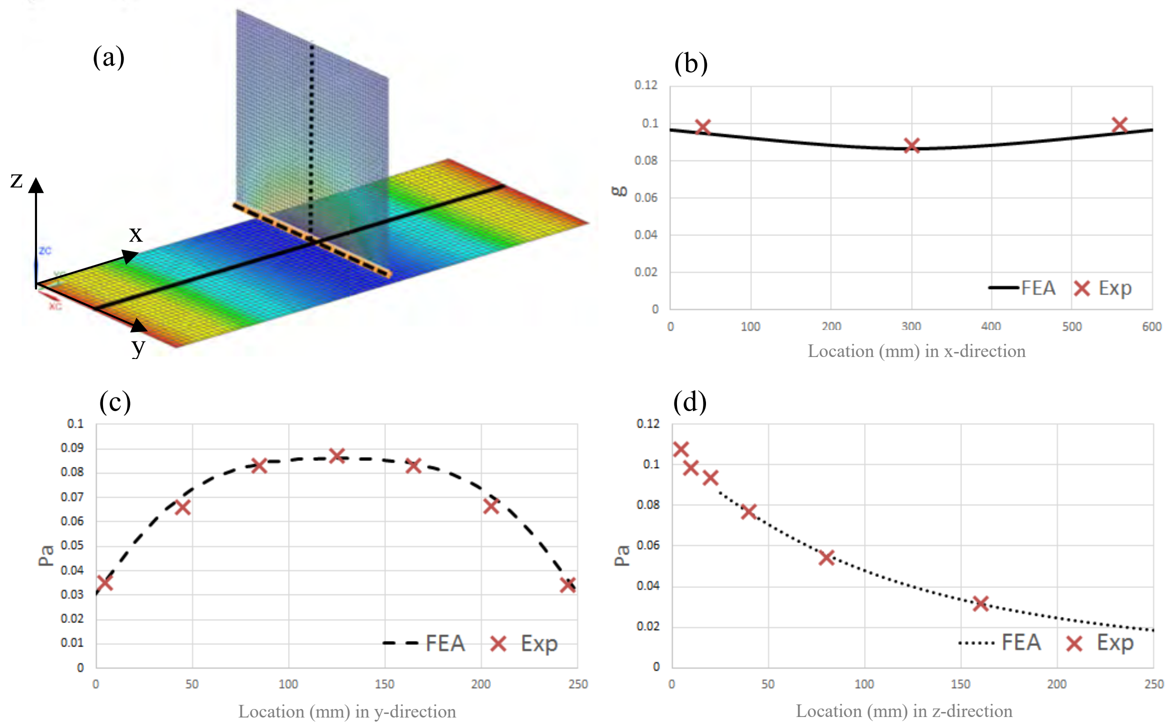

Figure 6. Plate in plate vibration at non-resonance mode (a) measurement locations, (b) plate acceleration, (c) acoustic pressure along the centre line and (d) acoustic pressure at different heights.

The second case of a vibro-acoustic plate FE/BE model validation is the plate vibrating at an anti-symmetric mode, 617 Hz third torsional normal mode, for both with and without localized damping. The localized damping location shown in figure 7(a). Figure 7(d) shows comparison between the relative phase results from FE/BE simulation and measurement, both methods show same trend. The most distortion of phase, comparing with undamped areas, can be observed at localized damping area.

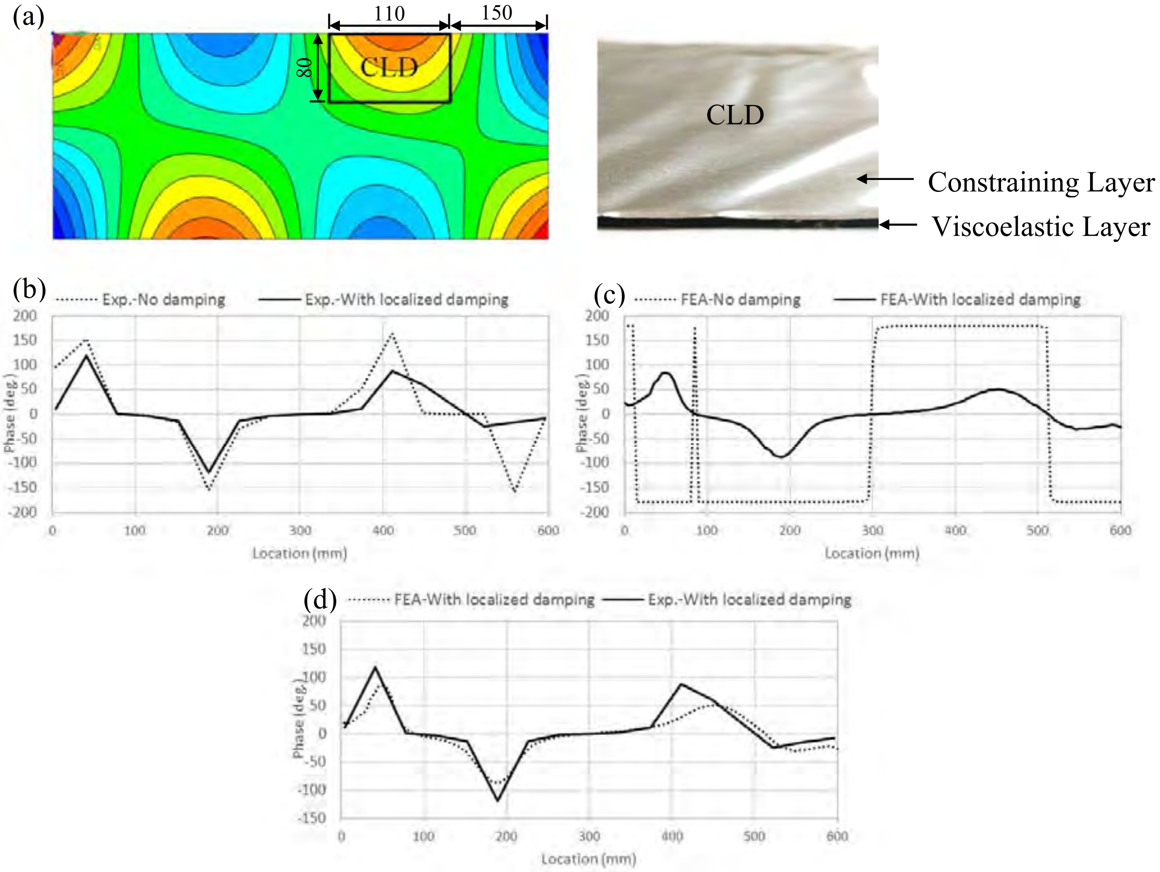

Figure 7. The relative phase between upper and lower line in nodal area of the plate vibrating at third torsional mode, for with and without localized damping.

Figure 8 shows the relative phase of nearfield acoustic at nodal area (solid line), nearfield acoustic at active area (dot line) and acceleration response at active area. The active area is the responses at the both longitudinal edge (x-direction) of the plate. The phase distortion at localized damping is clearly observed only on the nearfield acoustic at nodal area, while being merely observed on other cases. The wave propagating at active area is too strong to be affected by adjacent areas, while at nodal area is more sensitive to wave propagating from adjacent areas. The acceleration response of the plate is only from one local point, while the nearfield acoustic is response from both local and global areas so that the effect of complex mode is stronger.

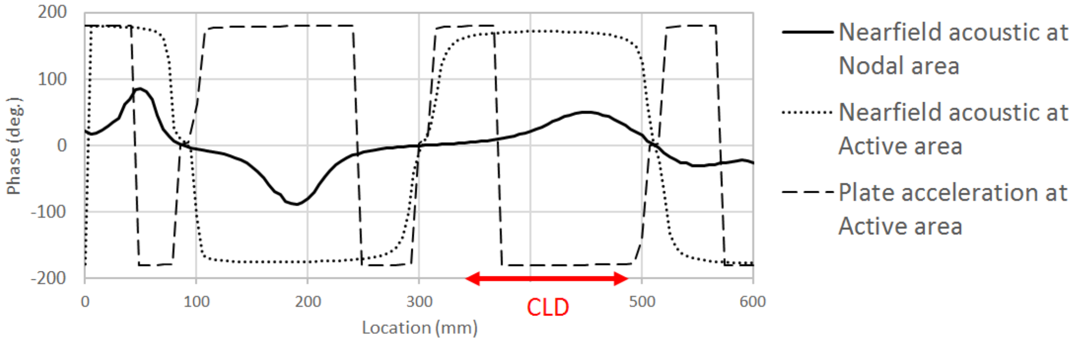

Figure 8. The relative phase of nearfield acoustic at nodal area (solid) and at active area (dot) and plate acceleration at active area (dash).

Table 1 shows the numerical results of nearfield acoustic on the several placement configurations of localized damping on a plate. The acoustic pressure and the pressure phase at nodal line area were distorted depend on both size and location of applied damping layer. Each damping configuration has the unique relative phase (solid line) distortion. Damp case 04 & 05 show larger area of localized damping results more relative phase distortion at nodal line area.

	Damp 00: No Damp	Damp 01: Full Plate	Damp 02: Cross-Length
Displacement	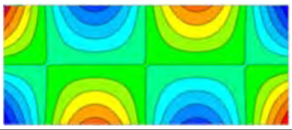	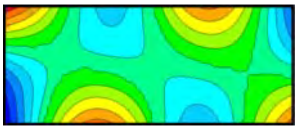	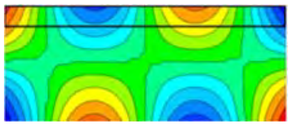
Acoustic pressure	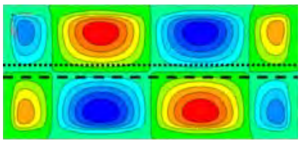	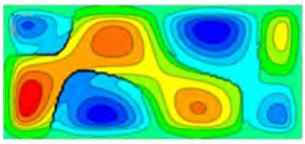	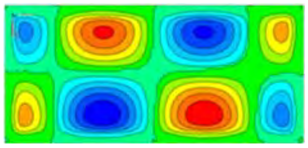
Acoustic pressure phase (deg.) Upper Line Lower Line Lower/Upper	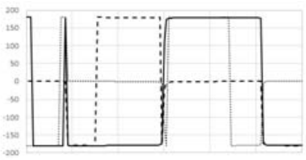	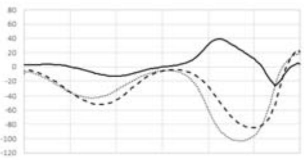	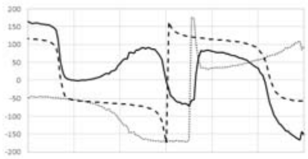
	Damp 03: Cross-Width	Damp 04: Partial-A	Damp 05: Partial-B
Displacement	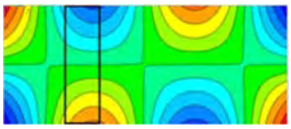	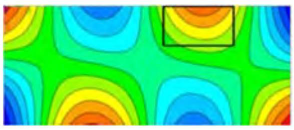	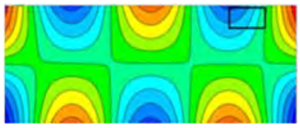
Acoustic pressure	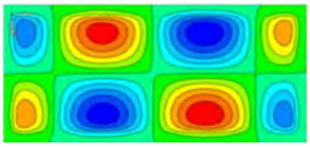	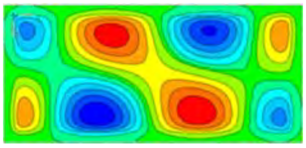	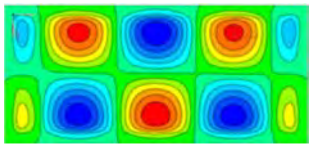
Acoustic pressure phase (deg.) Upper Line Lower Line Lower/Upper	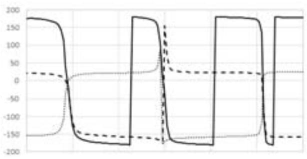	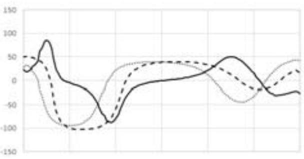	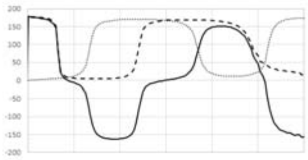

Table 1. The numerical results of nearfield acoustic on the several placement configurations of localized damping on a plate.

6. Conclusion

The localized damping identification method developed here is based on the requirement that the structure is vibrating at anti-symmetric mode. The present of localized damping lead to the occurrence of complex vibration modes, resulting the acoustic wave propagating from each area of the structure reach a nodal line at different instant of time. This distorts the phase of acoustic pressure at nodal line from identically 0° or 180°. The relative phase of a pair of microphone measure acoustic pressure was calculated, which is developed for output-only analysis and with single frequency excitation. It is shown that large distortion of the relative phase can be observed at localized damping locations. Each damping configuration has the unique distortion pattern, which depend on both size and location.

Future works will develop a method to extract damping ratio of the localized damping area using nearfield acoustic at nodal line, and the sufficient algorithm to accurately identify the damping locations of various configurations of damping treatments.

References

[1] E.M. Kerwin Jr, Damping of flexural waves by a constrained viscoelastic layer, *Journal of the Acoustical Society of America* 31 (1959) 952.

[2] D.H. Kruger, J.A. Mann III, T. Wiegandt, Placing constrained layer damping patches using reactive shearing structural intensity measurements, *Journal of theAcoustical Society of America* 101 (1997) 2075.

[3] Earl G. Williams, *Fourier Acoustics: Sound Radiation and Nearfield Acoustical Holography*, Academic Press, England, 1998.

[4] J.-T .Xing, W.G. Price, A mixed finite element method for the dynamic analysis of coupled fluid – solid interaction problems, *Royal Society: Mathematical and Physical Science* 433 (1888) (1991) 235 - 255.

[5] D.J. Ewins, *Modal Testing: Theory, Practice and Application*, second ed. Wiley, England, 2001.

[6] OliverUnruh, Influence of inhomogeneous damping distributionon sound radiation properties of complex vibration modes in rectangularplates, *Journal of Sound and Vibration* 377 (2016) 169-184.

[7] Y.F. Xu,W.D. Zhu, Operational modal analysis of a rectangular plate using non-contact excitation and measurement, *Journal of Sound and Vibration* 332 (2013) 4927-4939.

[8] W.D. Zhu, J.M. Liu, Y.F. Xu, H.Q. Ying, A modal test method using sound pressure transducers based on vibro-acousticr eciprocity, *Journal of Sound and Vibration* 333 (2014) 2728-2742.

[9] PCB Piezotronics, Inc., *Microphone Handbook: Test and Measurement Microphones*, Depew, NY.

[10] T. Caughey, M. O'Kelly, Classical normal modes in damped linear dynamic systems, *ASME Journal of Applied Mechanics* 32 (1965)583–588.

[11] F. Fahy, *Foundations of Sound and Structural Vibration*, 2nd ed. Elsevier Academic Press, London, England, 2007.

[12] G. Lang, Demystifying complex modes, *Sound and Vibration* 23 (1989) 36-40.

[13] H. Koruk, K.Y. Sanliturk, A novel definition for quantification of mode shape complexity, *Journal of Sound and Vibration* 332 (14) (2013) 3390-3403.

[14] Unruh, M. Sinapius, H. Monner, Sound radiation properties of complex modes in rectangular plates: a numerical study, *Acta Acustica United with Acustica* 101 (2015) 62-72.